minerals

MDPI

Article

REE-Rich Turonian Phosphates in the Bohemian Cretaceous Basin, Czech Republic: Assessment as Source of Critical Elements and Implications for Future Exploration

Khaldoun Al-Bassam *, Petr Rambousek and Stanislav Čech

Czech Geological Survey (CGS), 118 21 Prague, Czech Republic; petr.rambousek@geology.cz (P.R.); stanislav.cech@geology.cz (S.Č.)

* Correspondence: albassam703@gmail.com

Abstract: Numerous phosphate occurrences are located in the Bohemian Cretaceous Basin (BCB) of the Czech Republic, within the Cenomanian–Turonian sequences. Small phosphate occurrences have been reported in the Upper Cenomanian, Lower Turonian, and Upper Turonian marine glauconitic siliciclasts. The phosphates are generally <1 m thick, present as phosphatized hardgrounds, nodules, coprolites, skeletal remains, phosphatized shells, peloids, sponges, and tube-fills, associated with black mudstone and other siliciclasts. Only recently the critical elements have been highlighted in these phosphates. The present study covers eight of these occurrences and provides information on petrography, mineralogy, and chemical composition of major elements, trace elements, and stable isotopes. The phosphate mineralogy is comprised of carbonate-fluorapatite, associated with quartz, glauconite, smectite, kaolinite, and pyrite. Most of the phosphates are rich in organic matter. The phosphate chemistry is dominated by P_2O_5, CaO, F, Na_2O, SO_3, and CO_2. Minor amounts of SiO_2, Al_2O_3, K_2O, and MgO are found, related to quartz and alumino-silicate impurities. Evidence of fossil microbial structures is revealed. The indices derived from rare earth elements (REE) indicate phosphogenesis at various redox conditions, ranging from anoxic to oxic, whereas the carbon stable isotopes of the apatite suggest generally reducing conditions. The critical and other valuable elements found in these Mid-Cretaceous phosphates include P_2O_5 (18.9–26.76 wt. %), F (1.67–3.25 wt. %), REE (325–1338 ppm), Y (74–368 ppm), and U (10.4–37.9 ppm). The investigation of the Turonian phosphate occurrences show that those located at the base of the Bílá Hora Formation (earliest Turonian) are the most persistent in the southern margins of the BCB, and found in localities extending for about 200 km. They were developed at the onset of the Early Turonian global transgression and are strata-bound to the base of the Bílá Hora Formation. Future exploration for marine sedimentary phosphorites should focus on thicker and better developed deposits at the base of the Turonian sediments as the main target.

Keywords: REE; Turonian; marine phosphates; intracontinental basin; Czech Republic

Citation: Al-Bassam, K.; Rambousek, P.; Čech, S. REE-Rich Turonian Phosphates in the Bohemian Cretaceous Basin, Czech Republic: Assessment as Source of Critical Elements and Implications for Future Exploration. *Minerals* **2021**, *11*, 246. https://doi.org/10.3390/min11030246

Academic Editor: Argyrios Papadopoulos

Received: 1 February 2021
Accepted: 24 February 2021
Published: 26 February 2021

1. Introduction

Phosphate resources are limited in Europe and occur as small deposits hardly sufficient to meet the industrial demands of European countries. Most European Union (EU) countries import phosphate rocks to produce phosphate fertilizers. In 2017, approximately 5.5 million tons of phosphate rocks were imported to the EU for this purpose. It is estimated that a maximum of 334 tons of natural uranium could have theoretically been recovered from 2017 EU phosphate rock imports, but this could satisfy only 2.1% of EU needs [1].

Moreover, it is well known that phosphate rocks are important sink for rare earths, uranium, and many other critical and valuable elements, but little is done in the EU countries to extract these metals as by-products during fertilizers' production. The European Commission recognizes the strategic importance of Critical Raw Materials (CRMs), which

are particularly important for technological progress, but sees no other choice than importing the ores and concentrates or the refined materials from other countries to feed its industrial needs [2].

In the Czech Republic, small phosphate occurrences have been reported in the Mid-Cretaceous sediments of the Bohemian Cretaceous Basin (BCB) by various authors [3–13]. Several phosphate-bearing horizons, associated with omission bioturbated surfaces, are known in the Upper Cenomanian sequence exposed at the Pecínov quarry (Pecínov Member of the Peruc-Korycany Formation) mostly present as scattered nodules and tube-fill deposits at omission surfaces [6,12]. Phosphate components are reported at the base of the Bílá Hora Formation (Lower Turonian) in many locations in the southern part of the BCB. They are present in various forms, such as phosphatized hardgrounds, nodules, sponges, skeletal bones, shark teeth, and tube-filled deposits [3–5,9,13]. Two phosphate marker beds are recognized at the base of the Upper Turonian Teplice Formation [7,14], where the phosphate components are comprised of coprolites and phosphoclasts. The phosphate occurrences of the BCB can be compared with numerous marine sedimentary phosphate occurrences reported in the Mid-Cretaceous (Albian–Turonian) marine sedimentary sequences in several European countries including Russia, France, Belgium, Germany, Poland, Hungary, Portugal, and Spain [15,16].

The present work includes compilation and analysis of all available information on previously and newly investigated phosphate occurrences of the BCB in the Czech Republic. It focuses on geology, petrology, geochemistry, metallogenesis, and assessment of the Cenomanian–Turonian phosphates in the BCB as potential resources of REE and other critical elements and to suggest a specific stratigraphic level for future exploration.

2. Geological Setting

The BCB (Cenomanian–Santonian) is an intracontinental depositional depression that formed by the reactivation of a fault system in the Variscan basement of the Bohemian Massif in the Mid-Cretaceous [6,17] and acted as a seaway between the North Sea and the Tethys Ocean. It extends from Brno in E Moravia across Bohemia to the N and W of Prague (Figure 1). Sedimentation within the BCB began during the late Albian or the earliest Cenomanian [18], and experienced several phases of development. The Cenomanian–Lower Turonian sequence in the BCB is represented by the Peruc-Korycany Formation (Cenomanian) and the Bílá Hora Formation (Lower Turonian). The Middle–Upper Turonian sequence is represented by the Jizera and Teplice formations [7,8,12,19]. The Peruc-Korycany Formation consists of three members: Peruc and Korycany members [19] and the Pecínov Member [20].

2.1. Lithostratigraphy of the Phosphate-Bearing Sequences

This is a summary of results obtained by various Czech geologists on the lithostratigraphy of the phosphate-bearing Mid-Cretaceous units in the BCB [7,8,10,19–21]. The Mid-Cretaceous phosphate occurrences of the BCB are mainly found in the Upper Cenomanian (Pecínov Member of the Peruc-Korycany Formation), Lower Turonian (Bílá Hora Formation), and Upper Turonian (Teplice Formation) (Figure 2).

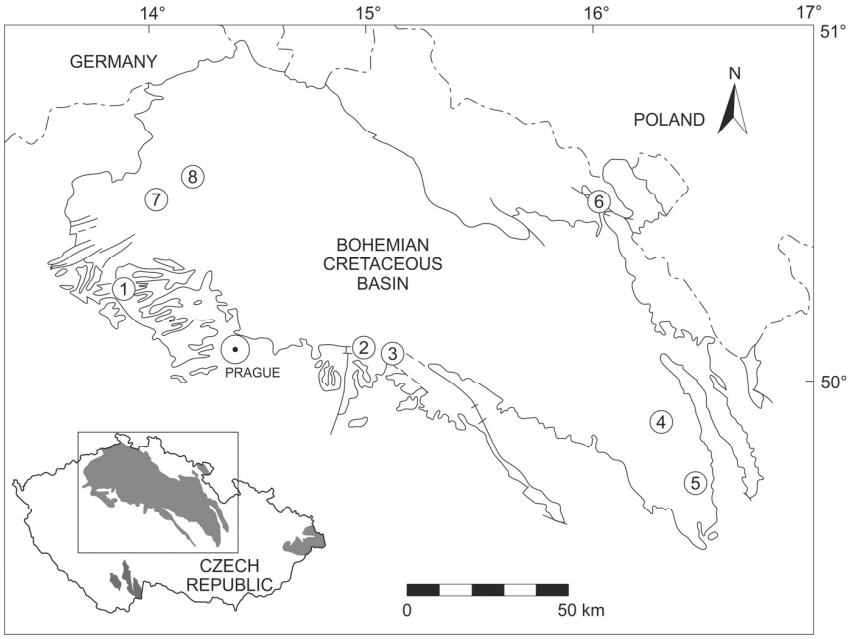

Figure 1. Map of the Bohemian Cretaceous Basin showing the location of the Cenomanian–Turonian phosphate-bearing sections: (1) Pecínov quarry, (2) Plaňany quarry, (3) Nová Ves quarry, (4) Česká Třebová "Třebovské stěny", (5) Březinka–Chvalka, (6) Rtyně v Podkrkonoší, (7) Úpohlavy quarry, and (8) Býčkovice road-cut.

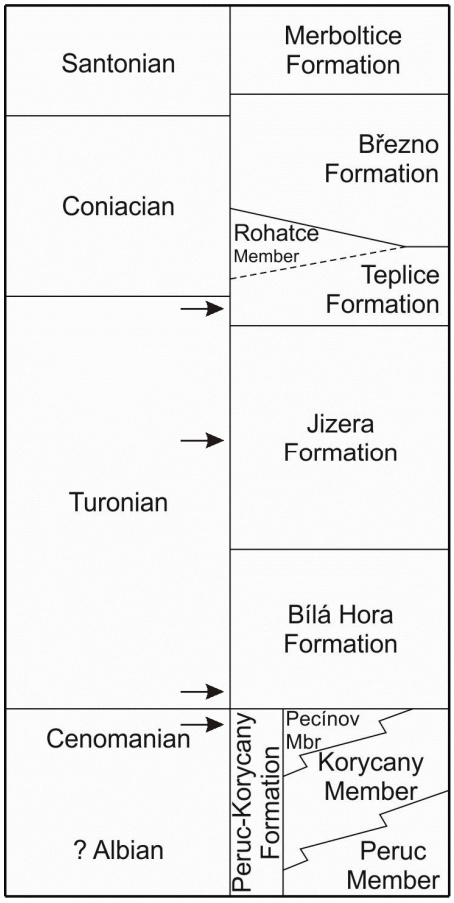

Figure 2. Stratigraphic sequence of the Bohemian Cretaceous Basin (Adopted from Reference [22] after References [19,20]. Arrows added to mark phosphate occurrences in the sequence.

2.1.1. Peruc-Korycany Formation (Cenomanian)

Peruc Member: The lower part consists of fining upward cycles of gray sandstones and conglomerates, interbedded with gray mudstones. The upper part contains gray sandstones and conglomerates, but is dominated by mudstones with root zones and carbonaceous plant debris. The uppermost part consists of finely laminated black mudstones with lenses and interbeds of glauconitic siltstones and fine-grained sandstones.

Korycany Member: It consists of well-sorted fine and medium grained quartzose sandstones and clayey sandstones. The sandstones contain locally high content of glauconite, thin layers of plant material, and mud drapes. The sequence suffered intensive bioturbation. In the middle and upper parts, a thin heterolithic facies was observed and, in some wells, a thin pebbly bed in the middle part with an erosive base is noticed.

Pecínov Member: It consists of gray-to-dark-gray glauconitic mudstones with varying silt content, locally containing fine sand. Pyrite concretions, a few mm to 3 cm in size, and some phosphate nodules, are scattered throughout the thickness of the unit. Uličný [6] divided the Pecínov Member into four principal units (P1–4). The units are bounded by well-recognizable, erosional, and/or burrowed surfaces, often filled with phosphate mineralization.

2.1.2. Bílá Hora Formation (Lower Turonian)

The open sea facies of the Early Turonian overly the Upper Cenomanian inner shelf facies by a prominent erosive surface and gap in sedimentation, which is associated with stratigraphic condensation, is represented by the abundant glauconite and phosphate at the base of the Bílá Hora Formation. It is comprised of dark-gray-to-gray marlstone and limestone. Glauconite occurs at the base of the formation as thin, green, silty mudstone (Unit BH1 at the Pecínov quarry). The basal part of the Bílá Hora Formation is characterized by abundant phosphates as dark brown nodules, skeletal clasts, sponges, and tube-fills. In the SE part of the BCB, phosphatic bioturbated hardgrounds mark the base of the Bílá Hora Formation.

2.1.3. Jizera and Teplice Formations (Middle–Upper Turonian)

The exposed sequence of the Jizera and Teplice formations at the Úpohlavy quarry consists of marls, fossiliferous clayey limestone, and marl/limestone alternations [14]. Two phosphate coprolite-bearing marker beds with shark teeth are reported at the base of the Teplice Formation in several localities [7,10,14]. The boundary between the Jizera and Teplice formations is taken at the Lower Coprolite Bed, which defines the base of the Teplice Formation. At the Úpohlavy quarry, it is 20–30 cm thick, glauconitic with mm's-sized quartz grains, and bored phosphate clasts. The coprolite-bearing beds are overlying an erosive base marking the upper boundary of the offshore Jizera Formation with the hemipelagic Teplice Formation and they can be traced in neighboring localities [10]. Some minor showings of phosphate intraclasts are found in this work in the Jizera calcareous rocks at Rtyně v Podkrkonoší locality.

3. Samples and Methods

Eight phosphate occurrences have been studied in this work (Figure 1 and Table 1). The phosphate occurrences are of Lower–Upper Turonian age. More than 100 samples were collected and examined from these occurrences. The results are kept in the archives of the Czech Geological Survey (CGS) and most of them are included in recently published papers [11,13,23,24]. All laboratory work was performed at CGS. The samples were examined and described under a polarized-light optical microscope and their mineral phases were determined by X-ray diffraction (XRD) following routine procedures of CGS laboratories. Powder XRD patterns of whole-rock samples were collected on Bruker D8 Advance diffractometer Bragg-Brentano geometry, using Cu $K\alpha$ radiation and Lynx Eye XE detector. Structural CO_3 content in carbonate-fluorapatite was determined (as CO_2 wt. %) from the XRD scans following the Gulbrandsen [25] method. Chemical analysis of major oxides was

carried out following conventional wet chemistry procedures of CGS [26]. Trace element concentrations were measured using an Agilent 7900× ICPMS, housed at CGS. Basalt BHVO-2 (USGS) and phosphate-rich sample IC10D [27] were measured for monitoring the instrumental bias and assessing the quality control. Detailed petrographic examination and chemical microanalyses of selected samples were carried out on carbon-coated polished sections using an FEG-SEM Tescan MIRA 3GMU scanning electron microscope (SEM) supplied with energy dispersive spectrometer (EDS). SEM imaging mode as well as EDS analysis was conducted under the conditions of 20 kV accelerating voltage, 1 nA probe current, and WD of 8 mm.

Table 1. Turonian phosphate occurrences reported in the present work.

Locality	Coordinates	Lithology	Stratigraphy
Pecínov quarry	N 50.12933 E 13.91716	Phosphate nodules, phosphate molds, and skeletal remains in black and dark gray glauconitic mudstone.	Lower Turonian: Base of Bílá Hora Formation overlying Pecínov Member.
Planany quarry	N 50.05166 E 15.01666	Reworked phosphoclasts of sponges, intraclasts, skeletal remains, sponges, and tube-fills.	Lower Turonian: Base of Bílá Hora Formation overlying Kutna Hora Complex.
Nová Ves quarry	N 50.05533 E 15.13183	Phosphoclasts of shark teeth, sponges, intraclasts, and tube-fills topping hardground.	Lower Turonian: Base of Bílá Hora Formation overlying Korycany Member.
Česká Třebová	N 49.95933 E 16.50033	Phosphate tube-fills and phosphate cement in varicolored bioturbated and glauconitic silty nodular hardground.	Lower Turonian: Base of Bílá Hora Formation overlying Korycany Member.
Březinka–Chvalka	N 49.63400 E 16.59017	Dark brown phosphate nodules and tube-fills in sandy bioturbated and glauconitic hardground.	Lower Turonian: Base of Bílá Hora Formation overlying Korycany Member.
Rtyně v Podkrkonoší	N 50.51450 E 16.06800	Dark brown angular phosphate intraclasts and skeletal remains in silty, recrystallized limestone.	Middle–Upper Turonian, Jizera Formation?
Úpohlavy quarry	N 50.46650 E 14.06416	Dark brown phosphate coprolites, tube-fills, and fish scales in dark gray lime-mudstone	Upper Turonian: Base of Teplice Formation, Lower Coprolite Bed.
Býčkovice road-cut	N 50.55117 E 14.22050	Phosphatic sponges, tube-fills, and intraclasts in lime-mudstone	Upper Turonian: Base of Teplice Formation.

4. Petrology

4.1. Petrography

The phosphates are associated with black glauconitic mudstone (Pecínov quarry), reworked heterogenic intraclastic phosphatic and calcareous deposits (Planany and Nová Ves quarries), and with dark gray glauconitic marl (Úpohlavy quarry). The macro phosphate components are present in various forms. The most common are nodules, several centimeters in size, usually brown in color (Figure 3A), coprolites, up to several centimeters long and 1 cm in diameter, brown and often show convolutions (Figure 3B), tube fills, several centimeters long, and 1–2 cm in diameter (Figure 3C) and phosphatized internal molds of bivalves (Figure 3D).

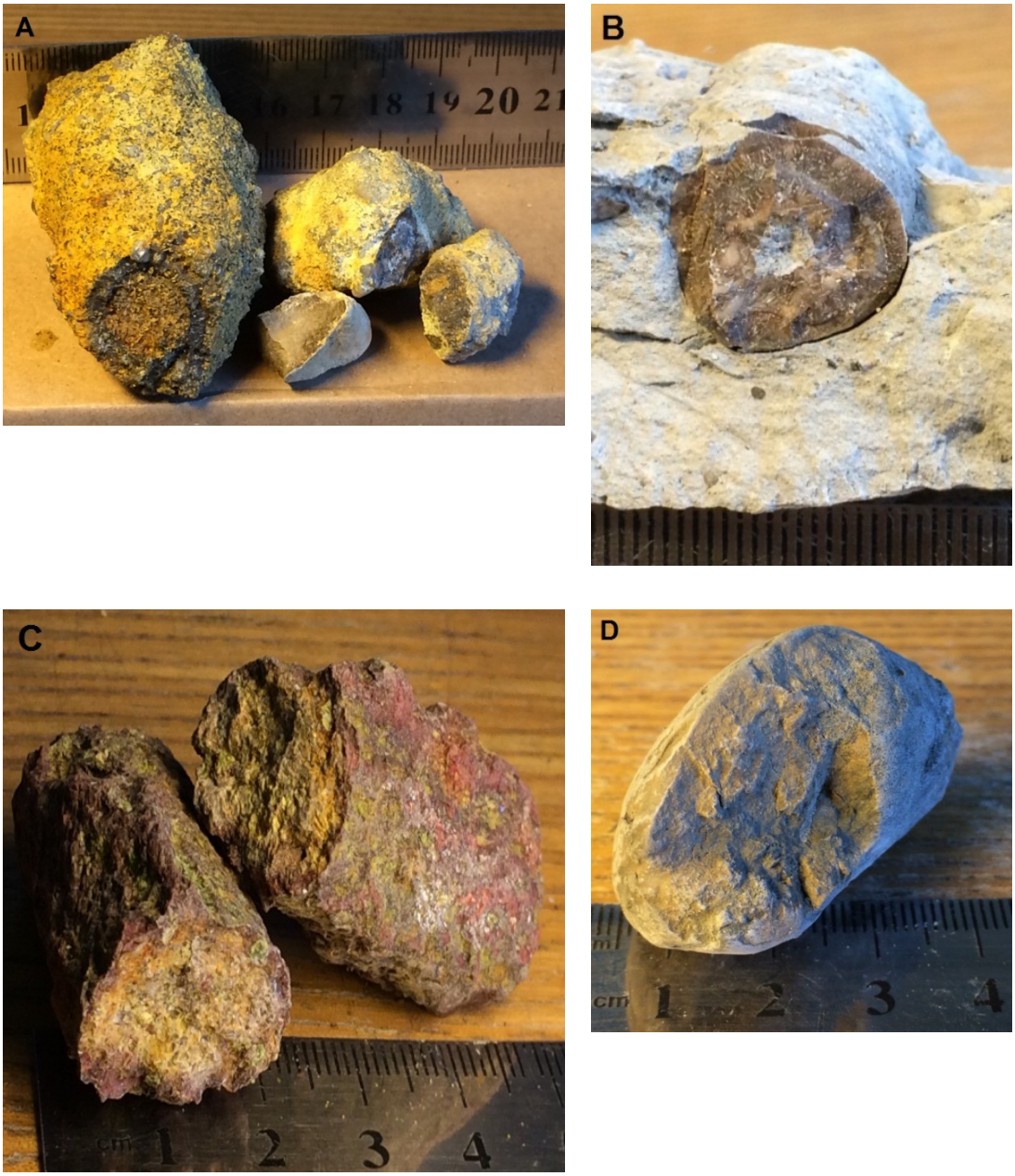

Figure 3. Phosphate components at the base of Bílá Hora Formation. (**A**) Phosphate nodule and tube-fills in hardground (Březinka–Chvalka), (**B**) Phosphate coprolite (Úpohlavy quarry), (**C**) Phosphate tube-fill (Planany quarry), and (**D**) Phosphatized bivalve mold (Pecínov quarry).

The micro-phosphate components are present as peloids, skeletal grains, fish teeth, intraclasts, sponges, and as cementing material, mostly associated with glauconite in siliciclastic sediments. The phosphate in the nodules and in the cement appears as cryptocrystalline brown material with abundant pyrite, silt-size quartz (<0.1 mm) and glauconite grains (~0.1 mm) (Figure 4A). Phosphatized bivalve shell fragments, brown, up to 1 mm long (Figure 4B), phosphatic angular skeletal fragments, 0.1–0.2 mm in size, and phosphatized sponges are common. Phosphate peloids (Figure 4C) and phosphate intraclasts are scarce (Figure 4D). Phosphate cement is found in sandstone (Figure 4E) and in the hardgrounds. Phosphate coprolites contain relatively less mineral impurities, but are richer in organic matter (Figure 4F). The phosphate coprolites and nodules often show microbial structures of <3 μm in size, interpreted as phosphatized fossil bacteria [23] (Figure 5A–D).

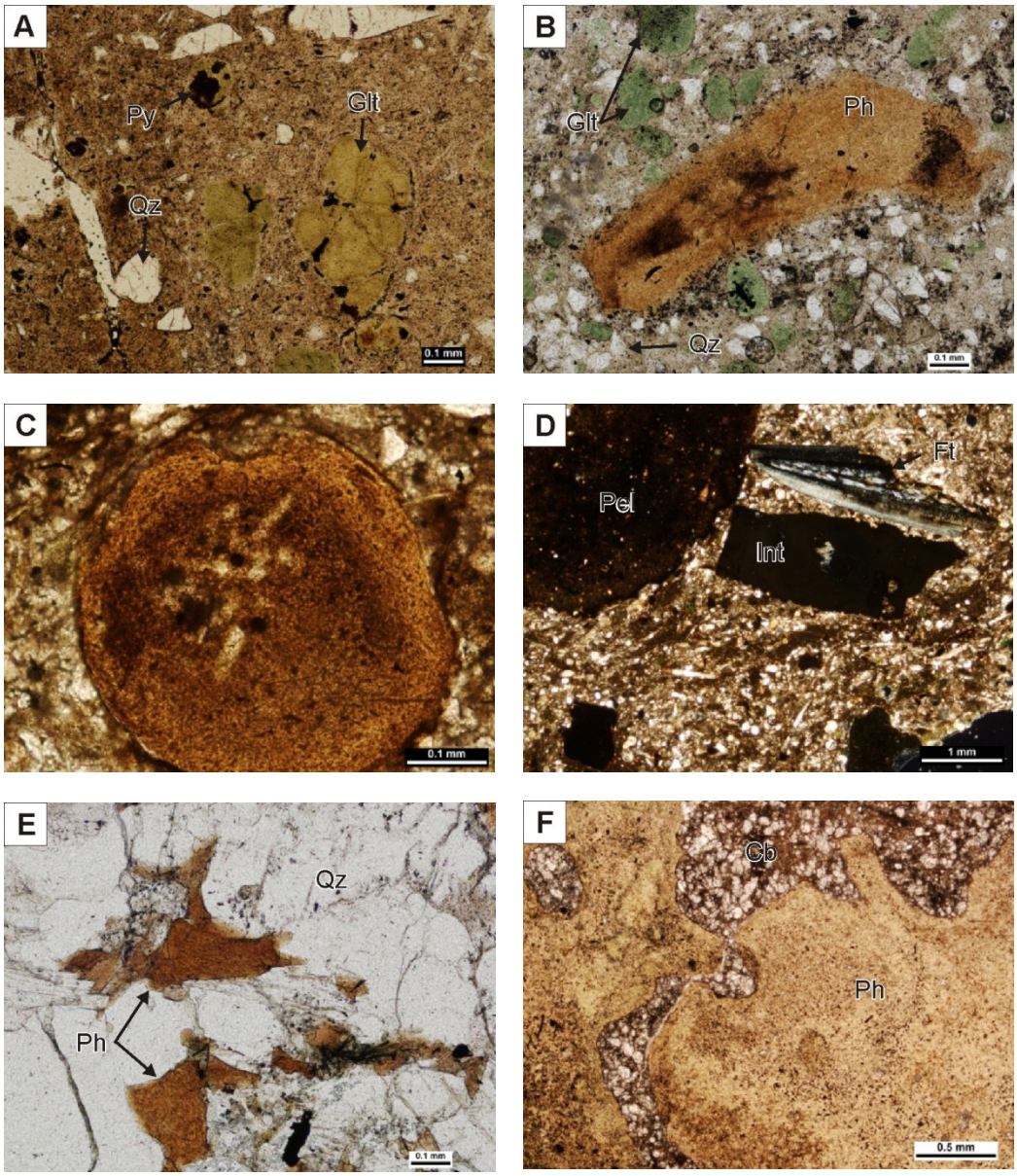

Figure 4. Microscopic textural components. (**A**) Cryptocrystalline apatite of phosphate nodule (brown) showing glauconite pellets (Glt) with pyrite inclusions (Py) and detrital quartz (Qz), (PPL). (**B**) Phosphatized shell fragment (Ph) in calcareous and fossiliferous matrix containing detrital quartz (Qz) (PPL). (**C**) Phosphate peloid (PPL). (**D**) Phosphate peloid (Pel), phosphate intraclasts (Int), and phosphate fish teeth (Ft) in glauconitic mudstone (XN). (**E**) Phosphate cement (Ph) in quartzose sandstone (Qz). (**F**) Fragments of phosphate coprolite (Ph) in carbonate matrix (Cb) (XN).

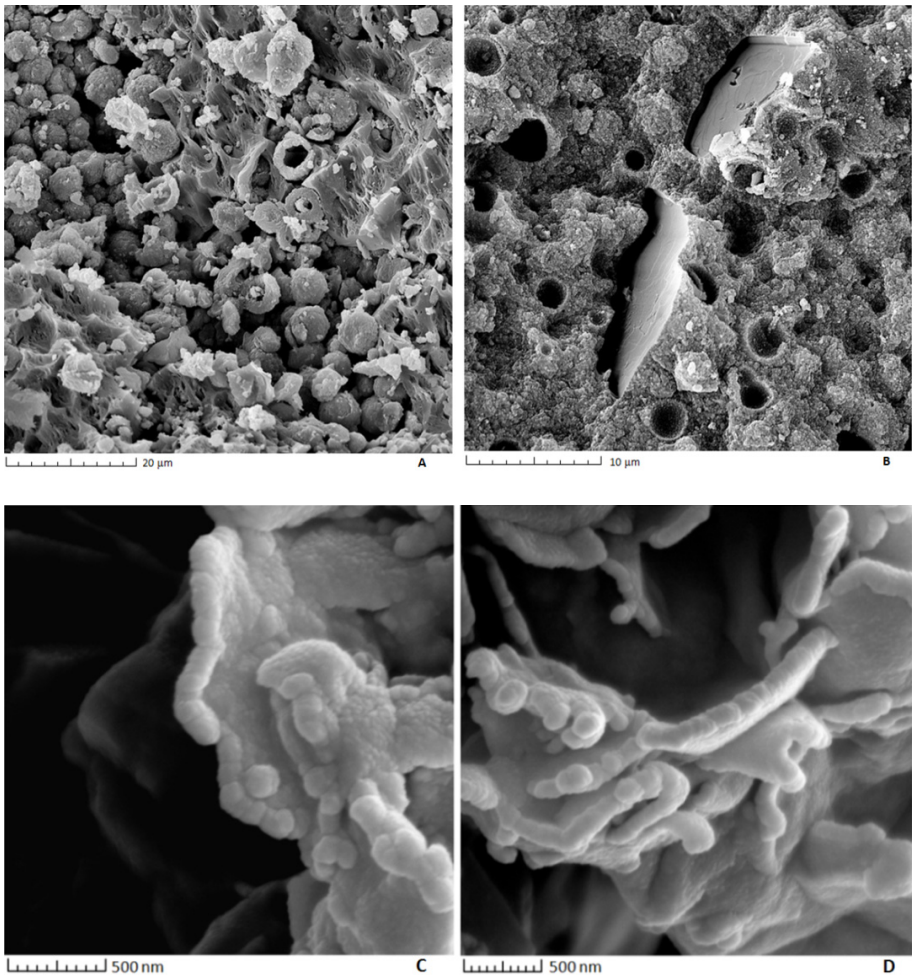

Figure 5. SEM images: (**A**,**B**) Cyanobacteria in phosphate coprolites. (**C**,**D**) Sulfur-reducing bacteria in phosphate nodules (adopted from Reference [23] with minor modification).

4.2. Mineralogy

Carbonate-fluorapatite is the major mineral in the phosphate nodules, coprolites, and other phosphate samples, as shown in the XRD analysis (Figure 6A). Other mineral associations identified by optical microscopy are inclusions of quartz, glauconite, and pyrite. The CO_3 content in the carbonate-fluorapatite structure, determined from the XRD spectra [25], is highly variable and reach up to 7.6 wt. % CO_3, which is higher in the phosphate nodules and coprolites. The mineralogy of the mudstone and sandstone host rocks in the Pecínov Member and Bílá Hora Formation are glauconite, quartz, pyrite, smectite, and kaolinite (Figure 6B). Occasionally, K-feldspar and gypsum are found in the siliciclasts. Calcite is found as a major mineral in the clastic components at the base of the Bílá Hora Formation in the sections of Plaňany and Nová Ves quarries and as lime-mudstone and calcareous fossil shells in the Lower Coprolite Bed of the Teplice Formation at the Úpohlavy quarry and Býčkovice road-cut sections.

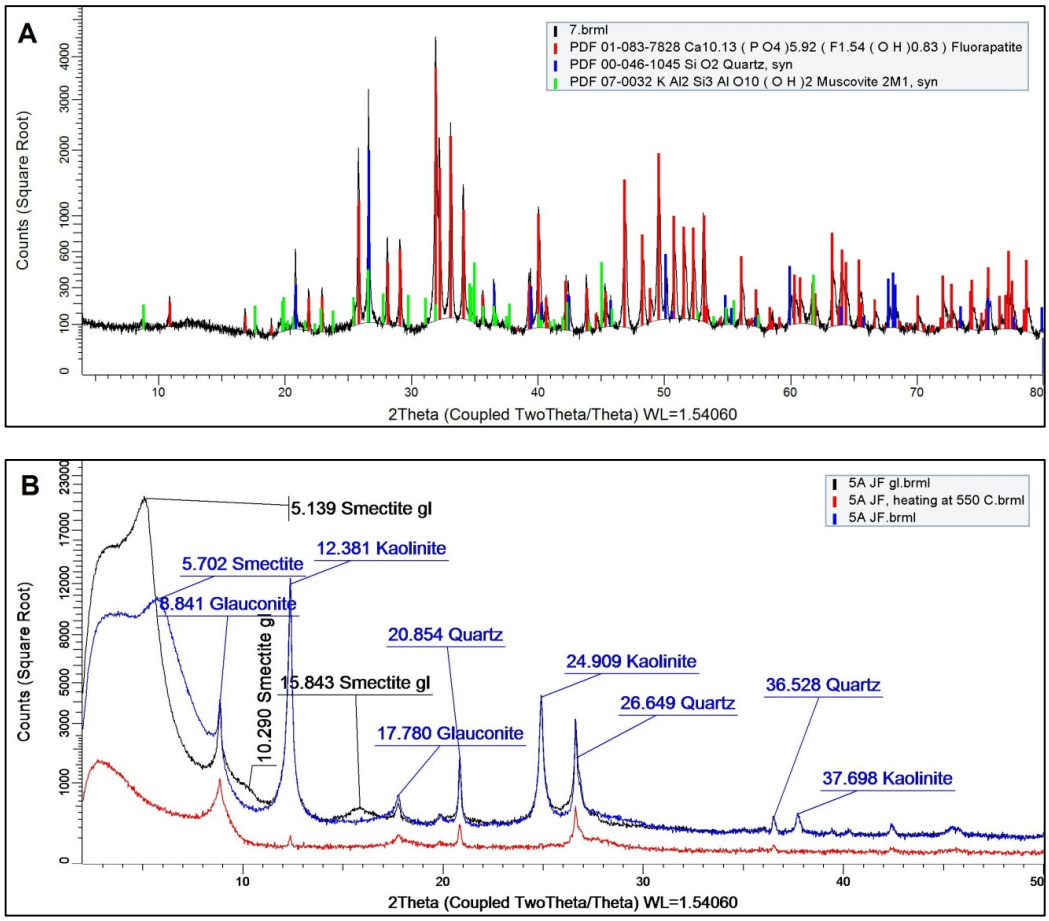

Figure 6. X-ray diffractograms of (**A**) phosphorite tube-fills in hardground at Česká Třebová locality (present work) and (**B**) black mudstone (−2 μm fraction) at the Cenomanian/Turonian boundary in the Pecínov quarry (adopted from Reference [13]).

5. Chemical Composition

5.1. Major and Trace Elements

The EDS analysis of apatite (Table 2) show P_2O_5, CaO, F, SO_3, Na_2O, and SrO as the major oxides with minor contents (<3.5 wt. %) of $\sum SiO_2 + Al_2O_3 + MgO + K_2O + Fe_2O_3$, which are present in the quartz and glauconite micron-size inclusions. The highest P_2O_5 and SrO contents are found in the phosphate fish bones, coupled with the lowest F content. The CaO content is generally uniform at about 48 wt. %. The Na_2O ranges between 0.65 and 0.84 wt. % and the SO_3 content ranges between 1.38 and 1.68 wt. %.

The average chemical composition (wet analysis) of the phosphate samples collected from seven localities in the BCB (Table 3) is dominated by the major components of the apatite: CaO (29.83–51.13 wt. %), P_2O_5 (18.90–26.76 wt. %), F (1.67–3.25 wt. %), Na_2O (0.12–0.88 wt. %), and SrO (0.07–0.30 wt. %). The contents of SiO_2, Al_2O_3, Fe_2O_3, and K_2O reported in the phosphate analysis are present in the minute quartz and glauconite inclusions common in the phosphate components. All phosphate samples contain appreciable amounts of organic carbon (up to 0.88 wt. %) and sulfur (up to 1.29 wt. %).

The phosphate samples show a wide range of trace element concentrations (Table 4) and they are enriched in REE (325–1338 ppm), Y, (74–368 ppm), U (10.4–37.9 ppm), and Zn (up to 600 ppm) relative to country rocks. The concentrations of REE, Y, and Zn in these phosphates are within the upper range reported for many giant marine sedimentary phosphorites in the Tethyan region, e.g., Dj. Onk deposit of Algeria [28], Al-Kora phosphorite province in Jordan [29], and Akashat phosphorite deposit of Iraq [30], but the BCB phosphates are comparatively depleted in uranium.

The geochemical association of F and P_2O_5 is controlled by the phosphate mineralogy and is shown in the high correlation coefficient reported between the two (r = 0.9), which is expressive of the carbonate-fluorapatite phase [13]. The geochemical affinity of REE, Y, and U toward apatite is well established [31]. These elements substitute for calcium (Ca^{2+}) in the apatite structure. In marine sedimentary rocks, carbonate-fluorapatite is considered the major sink of these elements. This geochemical affinity is demonstrated in the previous work of Al-Bassam and Magna [11] by the significant positive correlation coefficients (r > 0.7) of REE, Y, and U with P_2O_5. The highest correlation coefficient of REE is found with Y (r = 0.9), which is followed by U (r = 0.8).

Table 2. Average EDS microanalysis of the apatite in various phosphate components.

Wt. %	Nodules	Coprolites	Cement	Bioclasts
SiO_2	1.96	0.82	1.37	n.a.
Al_2O_3	0.85	0.26	0.49	0.12
Fe_2O_3	0.36	0.31	1.02	0.31
CaO	48.31	48.79	48.80	47.88
SrO	0.39	0.47	0.24	0.52
MgO	0.23	0.20	0.33	0.22
K_2O	0.17	0.16	0.38	n.a.
Na_2O	0.81	0.65	0.84	0.75
P_2O_5	31.14	31.73	30.76	36.61
SO_3	1.45	1.68	1.38	1.43
F	4.47	4.40	5.09	3.58

Table 3. Average major elements' chemical composition of the Turonian phosphates.

Wt. %	Pecínov Quarry (9 Samples) [1]	Nová Ves Quarry (3 Samples) [1]	Česká Třebová Quarry (2 Samples)[2]	Březinka Chvalka Outcrop (2 Samples) [2]	Úpohlavy Quarry (9 Samples) [1]	Býčkovice Road-Cut (1 Sample) [1]	Rtyně v Podkrkonoší (1 Sample) [2]
SiO_2	13.37	9.06	20.73	37.91	2.05	6.57	17.02
TiO_2	0.12	0.07	0.11	0.16	0.03	0.05	0.11
Al_2O_3	3.01	1.59	1.14	2.30	0.78	1.52	3.47
Fe_2O_3	2.13	1.24	2.56	1.87	1.19	1.71	2.50
FeO	0.42	0.20	0.36	0.45	0.18	0.21	0.22
MgO	0.54	0.45	0.47	0.35	0.34	0.44	0.56
MnO	0.018	0.025	0.015	0.023	0.017	0.019	0.035
CaO	40.77	47.32	39.56	29.83	51.13	50.30	38.41
SrO	0.197	0.200	0.072	0.085	0.304	0.15	0.099
Na_2O	0.88	0.59	0.12	0.32	0.52	0.47	0.21
K_2O	0.79	0.28	1.12	0.77	0.15	0.58	1.00
P_2O_5	23.67	26.01	26.76	18.90	25.14	24.90	25.91
F	2.74	2.85	2.26	1.67	3.25	2.83	1.84
CO_2	4.04	6.40	0.70	2.37	9.79	9.59	n.d.
C-organic	0.88	0.58	0.35	0.22	0.80	0.55	n.d.
S-total	1.29	0.28	0.09	0.20	1.26	0.22	n.d.
H_2O^+	3.56	1.70	2.18	2.15	0.40	n.d.	n.d.
H_2O^-	0.72	0.77	0.53	0.59	1.13	0.42	n.d.
-F equiv.	−1.153	−1.198	−0.950	−0.703	−1.369	−1.193	−0.775
-S equiv.	−0.322	−0.069	−0.023	−0.050	0.314	−0.055	-
Total	97.67	98.35	98.15	99.43	96.78	99.28	90.61

[1] [13], [2] Present work, n.d.: not determined.

Table 4. Average trace element concentrations of the Turonian phosphates.

Ppm	Pecínov Quarry (9 Samples) [1]	Nová Ves Quarry (3 Samples) [1]	Česká Třebová Quarry (2 Samples) [2]	Březinka Chvalka Outcrop (2 Samples) [2]	Úpohlavy Quarry (9 Samples) [1]	Býčkovice Road-Cut (1 Sample) [1]	Rtyně v Podkrkonoší (1 Sample) [2]
Sc	12.6	5.6	10.0	4.0	9.8	2.4	2.3
Cr	11.6	5.3	10.5	35.0	1.1	4.8	23.0
Co	3.8	3.7	7.0	4.0	6.0	3.0	n.d.
Ni	18.2	13.4	12.0	6.5	26.3	11.3	18.2
Cu	16.6	14.5	10.5	4.0	20.1	19.8	n.d.
Zn	60.3	17.8	23.0	14.5	599.9	12.8	n.d.
Rb	11.7	8.5	48.5	n.d.	3.6	8.8	n.d.
Y	213	74	548	131	368	144	153
Zr	40.3	16.6	45.5	151	47.4	22.5	18.1
Cd	0.07	0.12	3.0	3.0	0.74	0.12	n.d.
Ba	131	27.9	55.0	62.5	308	512	92.5
W	1.4	0.9	11.5	n.d.	1.0	1.0	n.d.
Pb	13.8	16.7	12.0	10.0	26.9	22.2	n.d.
Th	8.1	1.7	3.5	6.0	0.8	1.0	2.2
U	29.7	37.9	30.5	29.5	28.9	12.5	10.4
∑REE	873	325	1338	526	1300	529	n.d.
Ce-anomaly *	0.25	−0.06	−0.30	0.06	0.02	−0.12	-
Ce/La	4.84	1.58	0.84	2.58	1.88	1.28	-

[1] [11], [2] Present work, * Ce-anomaly = Log $\{3Ce_N/(2La_N + Nd_N)\}$ [32], REE normalized to Average Shale [33]. n.d.: not determined.

5.2. Critical Elements

According to the European Commission report [2], P, F, REE, and W are classified as Critical Raw Materials among other commodities. In this work, other elements of strategic importance are also highlighted and include U, Y, and Zr.

P_2O_5: The P_2O_5 content of the phosphate components is found to range from 19.6 wt. % to 26.5 wt. % in the phosphate nodules, 22.8 wt. % to 26.3 wt. % in the phosphatized coprolites, 24.9 to 28.5 in the phosphatized sponges, up to 28.6 wt. % in the phosphate nodules and tube-fills of hardgrounds, and up to 32.59 wt. % in the shark teeth, compared to 30–39 wt. % P_2O_5 in the carbonate-fluorapatite phase determined by EDS microanalysis of some phosphate samples (Tables 2 and 3).

F: The F content varies from 2.42 to 3.18 wt. % in the phosphate nodules and 2.86 to 3.50 wt. % in the phosphate coprolites, compared to 4.2 to 4.5 wt. % in the pure carbonate-fluorapatite, as shown in the EDS microanalysis (Table 2). The nodular phosphates in the hardgrounds show lower F content (1.50–2.57 wt. %) (Table 3) and up to 5.7 wt. % in the EDS analysis of the carbonate-fluorapatite (Table 2). The F content is directly proportional to the P_2O_5 content with F/P_2O_5 ratio of about 0.14, varying in a very narrow range in most samples, except in the nodular phosphate hardgrounds, where lower F content is noticed with the F/P_2O_5 ratio of about 0.10.

REE, Y, U, W, and Zr: Total REE concentration in the extracted phosphate samples reported by Al-Bassam and Magna [11] ranges from 631 to 1132 ppm in the phosphate nodules and 398 to 874 ppm in the phosphate coprolites. The partial analysis of REE (La, Ce, and Nd) in the new localities (Table 4) show elevated mean concentration of 1338 ppm in the phosphate samples of the Česká Třebová phosphate-bearing hardground compared to 526 ppm in the phosphate samples from the hardground at Březinka–Chvalka, in contrast to ∑REE of mostly <200 ppm in the associated siliciclastic samples [11]. Yttrium concentration ranges from 159 to 267 ppm in the phosphate nodules, 75 to 437 ppm in the phosphate hardground, and 152 to 475 ppm in the phosphate coprolites. Uranium concentration ranges from 20 to 38 ppm in the phosphate nodules, 26 to 37 ppm in the phosphatic hardgrounds, and 27 to 32 ppm in the phosphate coprolites. The highest U concentration of 43 ppm is found in the phosphatized sponges at the base of Bílá Hora

Formation. Relatively high W concentration of 20 ppm is found in the phosphate sample 60A collected from the hardground at Česká Třebová and elevated concentrations of Zr of 103–199 ppm are found in the phosphatic hardground at Březinka–Chvalka (Table 4).

5.3. Recovery of REE from Phosphates

The extraction of REE, U, and other valuable trace elements from phosphoric acid is a well-known world practice carried out during fertilizers production where they are recovered as by-products. The extraction these metals from phosphoric acid is considered an example of conservation of natural resources. If not recovered, they will be lost forever from the economy [34]. There is no experimental work on the recovery of REE, U, and other valuable metals from the Czech phosphates.

The world experience in this respect show that trace elements in the phosphate rocks are fractionated and partitioned over various products of the industrial stages of fertilizers production including beneficiation, production of technical or green phosphoric acid, fertilizers, and the wastes of phosphogypsum and slime [35,36]. Rare earth elements are only trace constituents of marine apatite, but as millions of tons of such apatite are dissolved annually to make phosphoric acid. The opportunity exists for increasing rare-earth output as a byproduct of fertilizer production [37]. Rare earth elements recovery from phosphoric acid was found more efficient in the HCl route of phosphoric acid production than the H_2SO_4 route of dissolution. Up to 80% recovery of REE has been reported, in laboratory experiments, using the former method [38]. However, it has been shown that REE in phosphorites are not totally transferred to phosphoric acid after acid dissolution. They are fractionated in various proportions among the main products of the fertilizer production system, including phosphoric acid, phosphogypsum, slime, mine tailings, waste clay, etc. [39].

6. Phosphogenesis

6.1. Main Phosphogenic Events in the BCB

The phosphate occurrences at the base of Bílá Hora Formation (earliest Turonian) are the most persistent in the BCB. They are present as a marker horizon, encountered in five sections, extending for about 200 km in a NW–SE direction along the southern margins of the BCB. These sections are Pecínov, Planany, Nová Ves, Česká Třepova, and Březinka–Chvalka (Figures 1 and 7). The phosphate mineralization is found at the basal part of the Bílá Hora Formation overlying, with a gap in sedimentation, various rock units. It is found on top of the crystalline rocks of the Kutná Hora Complex (Plaňany section), Korycany Member (Česká Třebová, Březinka–Chvalka, and Nová Ves sections), and Pecínov Member of the Peruc-Korycany Formation (Pecínov section) (Figure 7).

The Early Turonian phosphate mineralization is present as phosphate nodules in the Pecínov quarry, accumulation of phosphatized bivalve shells, skeletal remains, shark teeth, and phosphatized sponges in the Plaňany and Nová Ves quarries and as phosphatic and bioturbated hardground in the Březinka–Chvalka and Česká Třebová sections. The phosphate mineralization in these sections is associated with stratigraphic condensation, glauconite, omission surface, bioturbation, and hardgrounds. The phosphogenic event marks the onset of the Early Turonian global eustatic transgression in the BCB. The phosphate horizon at the base of the Bílá Hora Formation is thin, usually <1 m, and the lithology of the host rocks consists of black mudstones, siltstones, quartz-sandstone, bioturbated phosphatic, and silty mudstone hardgrounds, and/or a heterogeneous mixture of bioclasts and intraclasts. With the exception of phosphatic hardgrounds, the other phosphate components in this part of the sequence show evidence of reworking.

The basal part of the Teplice Formation (Upper Turonian) is marked by two remarkable beds of phosphatic marl, holding phosphatized coprolites, sponges, skeletal remains, and shell fragments. These basal phosphate-bearing glauconitic marl horizons are about 0.5 m in thickness at the Úpohlavy quarry and show evidence of sequence condensation. This phosphogenic event was also recorded at the Býčkovice outcrop [10] and is considered a

marker horizon, always found at the base of the Teplice Formation marking the contact with the Jizera Formation [7,14].

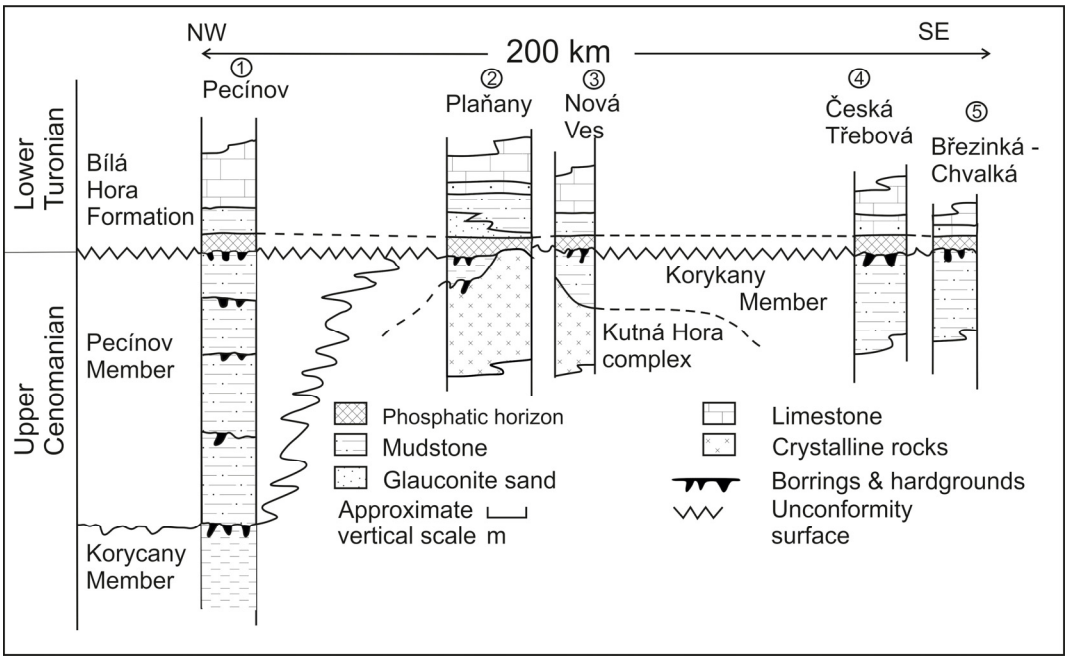

Figure 7. Stratigraphic correlation of the investigated Early Turonian phosphate occurrences of the Bohemian Cretaceous Basin (BCB) (See Figure 1 for geographic location).

6.2. Origin and Phosphogenic Environment

All phosphate occurrences covered by this survey are of marine sedimentary origin, mostly found in condensed and glauconitic sequences, omission surfaces, and bioturbated hardgrounds. The persistent phosphate mineralization at the latest Cenomanian/earliest Turonian coincides with the most pronounced anoxic event of the Cretaceous, which is well known as the Oceanic Anoxic Event 2 (OAE2). The initial source of phosphorus of these deposits is continental in origin, derived from deeply weathered felsic and intermediate igneous and older siliciclastic rocks, by rivers to the marine basin [13]. The local source was most likely P-rich organic matter and Fe-oxyhydroxides, derived to the basin from terreginous sources, and supplied phosphorus to the pore water environment.

Long periods of warm and humid climate during the Mid-Cretaceous, reported by various workers [40–42], enhanced weathering intensity of source rocks, indicated by mineralogical and geochemical criteria [13,24,43]. A warm and wet climate promotes chemical weathering and river input of phosphorus to the sea [44] and the onset of the C/T ocean anoxic event (OAE2) was triggered by a short-lived increase in phosphorus burial [45]. The authigenic marine precipitation of phosphates is generally accepted to take place in the reducing environment of the pore water, below sediment–water interface, following the bacterially-mediated liberation of phosphorus sorbed on Fe-oxyhydroxides and/or attached to organic matter [46–51].

A short-lived phosphogenic environment dominated the southern margins of the BCB at the Cenomanian/Turonian (C/T) boundary, associated with condensed and starved sedimentary sequence. The bio-stratigraphic hiatus at the Cenomanian/Turonian boundary has been recently confirmed [12]. The lithological break is marked by bioturbated phosphatic hardgrounds and/or their reworked derivatives, which are rich in glauconite and depleted in authigenic carbonates and found in all the studied sections along the southern margins of the BCB. Continuous subsidence of the BCB during the Cenomanian resulted in a depth increase and, as a consequence, eutrophication of subsurface waters. The rate of subsidence varied considerably within the BCB and was at its maximum in the N and NE parts of the

basin (Čech, 1993, in Reference [22]). In the vicinity of the Pecínov quarry, several meters of relatively deeper facies black and dark gray silty mudstones of the Pecínov Member were deposited on top of the Korycany Member. The deposition of these mudstones is restricted to the deeper, suboxic part of the BCB during Upper Cenomanian and is not found elsewhere in the basin, where the Turonian sediments of the Bílá Hora Formation overly the Korycany Member or even the Kutná Hora crystalline complex (Figure 7).

The Cenomanian drowning in the BCB ceased due to a global sea-level fall. A sequence boundary of latest Cenomanian age in the Pecínov section is correlated to a global sea-level fall during the *N. juddii* zone [6]. This was followed by a renewed sea-level rise that occurred during the early Turonian at the *W. coloradoense* zone and reached maximum flooding during the *M. nodosoides* zone [6]. As a result, a firm ground was developed and the consolidated deposits were penetrated by organisms producing *Thalassinoides* traces and an omission surface with a burrow system was formed. This was followed by hardground development, borings, and initiation of glauconitization and phosphatization processes, which led to the formation of a composite hardground.

It is shown that glauconite is a reliable indicator of condensed sections. Abundant glauconite may reflect marine transgression associated with sediment starvation [52,53]. It is found in intimate association with the phosphates at the C/T boundary in the BCB [13]. Marine phosphorites, associated with black shales, are suggested to correlate among other criteria, with the development of widespread oxygen-depleted waters induced by reduced rates of oceanic circulation and oxygen solubility, giving rise to the formation of phosphatic hardgrounds [54].

The phosphate deposits were reworked during a regional low-stand event of a sea level that caused erosion and discontinuity. The early stage of the Turonian transgression led to the reworking of these hardgrounds in many places, such as Pecínov, Planany, and Nová Ves sections, but they are preserved in some other sections such as Březinka–Chvalka and Česká Třebová sections. The phosphate nodules at the base of the Bílá Hora Formation in the Pecínov quarry section were initially precipitated in a lower stratigraphic horizon and later reworked and accumulated in the overlying sequence [11,13].

Redox conditions during phosphogenesis, suggested by Ce-anomaly values [32], ranged from anoxic in the NW part of the BCB (Pecínov section), dysoxic in the central part (Nová Ves section), and variable in the SE part from oxic (Česká Třepova section) to anoxic (Březinka–Chvalka section). Several evidences of anoxia are found in the phosphate nodules at the Pecínov section, including a positive Ce-anomaly (0.22–0.28) and high Ce/La ratio (3.9–5.8) [11], sulfur-reducing bacteria [23], and negative $\delta^{13}C$ values in apatite structural CO_3 (−1.23–−0.86‰ PDB) [24].

The clastic phosphate components, found at the base of the Bílá Hora Formation in the Nová Ves section, related to the same phosphogenic event, were deposited in dysoxic rather than anoxic environment. They show REE indices of a transitional zone between oxic and anoxic environments, where the Ce-anomaly mostly ranges between −0.1 and 0.0 and Ce/La ratio of ~1.6 [11]. Sponges, skeletal fragments, shark teeth, and shell fragments were phosphatized in dysoxic conditions and later suffered reworking in a shallow and more oxygenated marine environment that preceded the onset of the Early Turonian transgression (base of Bílá Hora Formation). On the other hand, the REE redox indices found in the hardground phosphates indicates variable redox conditions, ranging from oxic at Česká Třepova (Ce-anomaly ~−0.3 and Ce/La ratio = 0.84) and anoxic at Březinka–Chvalka (Ce-anomaly = 0.06 and Ce/La ratio = 2.6) (Table 4).

The Ce anomaly and Ce/La values found in the Early Turonian phosphates of the BCB are higher than those reported for oxic, open marine seawater of −0.76 and 0.35, respectively, [53] and suggest initial phosphate deposition in a restricted environment below a sediment-water interface. The REE pattern of distribution in the Early Turonian phosphate components, reported previously [11] and supported by the REE patterns of new results, show enrichment in the light REE (LREE) and, in some samples, a hump (bell-shape) in the middle REE (MREE). This pattern is well manifested in phosphate nodules at

the Pecínov section and suggests deposition in suboxic conditions below a sediment-water interface [32,55]. The intensity of the MREE enrichment correlates with the intensity of other REE redox indices of a Ce-anomaly and Ce/La ratio (Figure 8).

The Upper Turonian coprolitic phosphates at the base of the Teplice Formation mark another phosphogenic event that can be related to condensed sedimentation and low sea-level stand before the following transgressive cycle and the subsequent elevation of the sea-level [10]. The phosphate coprolites and other clastic phosphate components encountered at the base of the Teplice Formation in the Úpohlavy quarry and Býčkovice road-cut are clearly phosphatized fecal materials [10,13]. Phosphatisation of the initial coprolite fecal material took place under variable redox conditions, but more oxic than that of the phosphate nodules and other Early Turonian phosphates. This is indicated by the phototrophic type of fossil bacteria found in these coprolites [23], REE distribution pattern, and Ce-anomaly values, falling in the anoxic–oxic transitional zone [11].

Phosphatisation of the coprolites could have started below a sediment–water interface, where the process involved release of phosphorus entrapped in organic matter of the fecal material under suboxic conditions and subsequent phosphatisation of the coprolites with potential bacterial mediation [23]. The $\delta^{13}C$ values of the carbonate-fluorapatite structural CO_3, ranging from −1.68 to −1.83‰ PDB, support an initial suboxic environment of phosphatization [24]. The coprolites were reworked several times after phosphatisation and sustained contact with seawater for extended periods of time sufficient to incorporate higher concentrations of F, U, Y, Zn, and REE in the apatite structure.

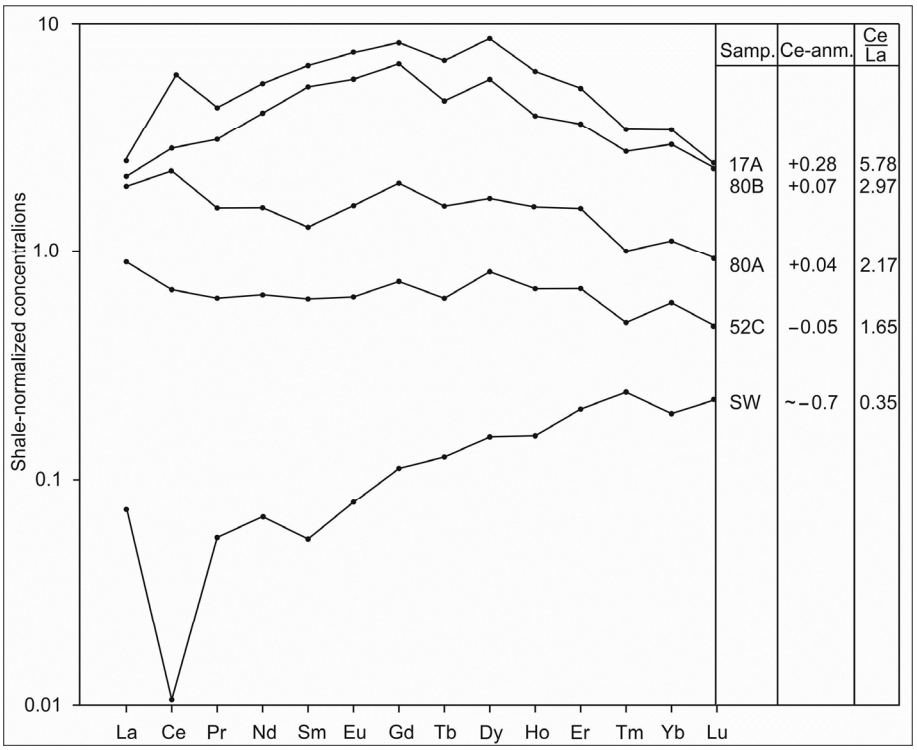

Figure 8. Rare earth elements distribution patterns in selected Early Turonian phosphate samples compared to seawater pattern. Sample 17A: phosphate nodule (Pecínov), data from Reference [11], Samples 80A and 80B: phosphate tube-fill (Březinka–Chvalka) (present work), Sample 52C: phosphatized carbonate clasts (Nová Ves), data from Reference [11], SW: seawater × 100, data from Reference [56].

6.3. Comparable Cretaceous Phosphogenic Events in Europe

Numerous Cretaceous phosphate occurrences have been reported in Europe, ranging in age from Albian to Maastrichtian [15]. The Late Cretaceous deposits are of the Tethyan

upwelling type and found in some Mediterranean European countries, extending in age from Upper Cretaceous to the Eocene. The Mid-Cretaceous phosphate deposits were developed in epicontinental seas and are of smaller extensions and thicknesses than the younger Tethyan deposits. The most common of these are minor phosphate occurrences reported in the Albian, Cenomanian, and Turonian sediments, mostly associated with discontinuity surfaces and reported in several countries of Europe.

The sequence described by Walaszczyk [57] at Annopol-on-Vistola section in Poland is comparable in age and phosphogenic events to the sequence of the Peruc-Korycany Formation of the BCB. The phosphate mineralization occurs at several discontinuity surfaces, especially at the Middle/Upper Cenomanian contact and Upper Cenomanian/Lower Turonian contact. The former is expressed by a composite hardground horizon, up to 30-cm thick, with glauconitic and phosphatic mineralization and may be compared with the omission phosphatic surface separating Unit P3 from Unit P2 of the Pecínov Member in the BCB. The latter discontinuity is reported by Walaszczyk [57] to represent a well manifested omission surface at the top of the heavily glauconitic Upper Cenomanian marls, equivalent in age to the omission surface between Unit P4 of the Pecínov Member (latest Cenomanian) and Unit BH1 (earliest Turonian) of the Bílá Hora Formation in the BCB.

Comparable age-equivalent phosphate occurrences are also reported in the Late Cenomanian sediments of the Russian Craton. Ilyin [58] reported that the Mid-Cretaceous Epicontinental sea covered the central part of the Russian Craton, which was differentiated into syn-sedimentary highs and lows. Condensed Cenomanian sequences were deposited, with abundant hiatuses, on the highs, crowned by an extensive phosphorite pavement, 30–50 cm thick. The phosphorite was described as a multi-layered phosphorite hardground, built of phosphorite nodules firmly cemented by a phosphate matrix. The nodules consist of phosphatized radiolarians, diatoms, and hexactinellid sponges [58]. Analyses show no carbonate in excess of what is substituted for PO_4^{3-} in the francolite structure. The delicate balance of the Cenomanian sea-level was abruptly interrupted by a major rise of sea-level, which happened around the Cenomanian/Turonian boundary and led to the drowning of the phosphate platforms and deposition of chalk [58].

Glauconite–phosphate association in hardgrounds was described from the Cenomanian of Devon, Southwest England [59]. The mineralization was classified into different groups on the basis of petrography and chemical analysis. Strong association between glauconite and phosphate was reported on a sub-microscopic scale. Glauconite and phosphate formation are believed to have taken place in the transitional zone between oxic and anoxic environments (suboxic zone). Iron oxyhydroxides were reported as a potential source of phosphorus and iron [59].

"Extensive" horizons of phosphatic rock of Turonian–Campanian age were discovered in the uppermost 10–25 m of the Vigla Formation in Greece. Some interesting uranium-bearing francolites have been reported in organic-rich phosphatic limestones from Greece by references [60,61]. Nodular phosphatic beds also occur in Germany where the "most extensive" of phosphate rocks are found in the Middle and Upper Cretaceous sediments in Mecklenburg. Phosphate nodules in Mid-Cretaceous glauconitic marl were reported in Hungary, extending for 43 km^2 [15].

7. Potential Phosphorite Exploration Targets in the BCB

The previous and new findings show that the phosphate-bearing horizon at the base of the Bílá Hora Formation, dated as Early Turonian, is encountered in all the localities investigated along the southern margins of the BCB [3–6,8,10,13,22]. This phosphate horizon is recorded in minor occurrences within a 200-km long belt extending from NW to SE along the southern margins of the BCB (Figure 7). It appears to be the most persistent Mid-Cretaceous marine sedimentary phosphogenic event known until now in the Czech Republic. It is also recorded in some European countries, such as Poland [57] and Russia [58], which may suggest a regional, short-lived, Mid-Cretaceous phosphogenic event in Europe.

The phosphates are situated at the base of the Bílá Hora Formation (Lower Turonian), overlying unconformably various rock units and marking the Early Turonian transgressive cycle in the BCB. However, despite the consistency of this phosphogenic event, the investigated Early Turonian phosphate occurrences are present in thin horizons and cannot be categorized as deposits in the economic sense, but, certainly, they are occurrences of great scientific significance. Most of the extracted phosphate components contain anomalous concentrations of REE and some other critical elements [11].

The phosphate-bearing horizons, documented until now in the Mid-Cretaceous sequences of the BCB, are mostly <1 m, in all the sampled localities. The bulk rock grade is generally low, not exceeding 5 wt. % P_2O_5. The phosphate components, mostly with >25 wt. % P_2O_5, are diluted by various lithologies of the host rocks, including mudstones, sandstones, and carbonates. Open cast, specific mining of these phosphates is economically not feasible due to the high stripping ratio and low P_2O_5 grade of bulk rocks, but, when the country rocks are excavated for other purposes, such as raw material for the cement industry (e.g., Pecínov quarry), the Early Turonian phosphates (base of Bílá Hora Formation), which are part of the overburden, can be excavated by selective mining and concentration by physical methods. However, this does not exclude the possibility of discovering thicker phosphate horizons of higher P_2O_5 grade in the Early Turonian sequence after detailed exploration.

Based on the results presented in this study, the Early Turonian phosphate-bearing horizon can be recommended as the main exploration target for marine sedimentary phosphorites in the BCB. The future exploration work should focus on discovering reasonably sizable and high-grade phosphate deposits of economic importance as source of REE and/or other critical and valuable metals. Such targets may be found in the undisturbed pristine phosphate hardground similar to that at Česká Třebová. However, large phosphate deposits should not be expected since this interval of the Cretaceous Period (Turonian) is not known as a large-scale phosphogenic period in the world. The giant Cretaceous phosphorite deposits are of a younger age, spanning across the Campanian to the Maastrichtian and even younger to the Paleogene, and were deposited in the Neo Tethys oceanic upwelling sedimentary regime [15,62,63].

8. Conclusions

Several short-lived phosphogenic events are recorded in the Turonian marine sediments of the BCB. They are occasionally present as pristine nodular phosphate hardground, but more often as reworked phosphoclasts. They are associated with glauconite, condensed sections, and suboxic environments. High concentrations of critical and other valuable elements in the Turonian phosphates include P, F, REE, Y, U, and W. The Early Turonian phosphate horizon is the most persistent among the Turonian phosphates. It marks the Early Turonian global transgression, stratigraphically bound to the base of the Bílá Hora Formation and overlying, with a break in sedimentation and various geological units. This strata-bound phosphate horizon can be recommended as a future exploration target for marine sedimentary phosphorites in the southern margins of the BCB.

Author Contributions: Conceptualization, K.A.-B. Funding acquisition, P.R. Investigation, S.Č. and P.R. Writing—review & editing, K.A.-B. All authors have read and agreed to the published version of the manuscript.

Funding: This project is funded by the Czech Geological Survey, Czech Republic.

Institutional Review Board Statement: Not applicable.

Informed Consent Statement: Not applicable.

Data Availability Statement: All data are uploaded to European project FRAME, WP4 database and most of original raw data are already published (please see Al-Bassam and Magna, 2018; Al-Bassam and Halodová, 2018, Al-Bassam, 2018 and Al-Bassam et al., 2019).

Acknowledgments: The present work is supported by the Czech Geological Survey (CGS) and it was initially prepared as part of the CGS contribution to the European project FRAME-WP4. Thanks are due to František Laufek for the XRD analysis and to Jiří Frýda and Vera Zoulková for chemical analysis.

Conflicts of Interest: The authors declare no conflict of interest.

References

1. Tulsidas, H.; Gabriel, S.; Kiegiel, K.; Heneklaus, N. Uranium resources in EU phosphate imports. *Resour. Policy* **2019**, *61*, 151–156. [CrossRef]
2. European Commission. *Report on Critical Raw Materials in the Circular Economy*; European Commission: Brussels, Belgium, 2018.
3. Žítt, J.; Nekvasilová, O. New occurrences of phosphorites in the Upper Cretaceous of the Prague and Kolín lithofacial regions (Czechoslovakia). *Bohemia Cent.* **1992**, *21*, 5–18.
4. Žítt, J.; Nekvasilová, O. Epibionts, their hard-rock substrates, and phosphogenesis during the Cenomanian-Turonian boundary interval (Bohemian Cretaceous Basin, Czech Republic). *Cretac. Res.* **1996**, *17*, 715–739. [CrossRef]
5. Laurin, J. Sedimentary Discontinuities with Evidences of Phosphatic Mineralization as a Record of the Changes of Sea Level; Bohemian Cretaceous Basin. Master's Thesis, Charles University, Prague, Czech Republic, 1996; p. 122. (In Czech).
6. Uličný, D.; Hladíková, J.; Attrep, M.J., Jr.; Čech, S.; Hradecká, L.; Svobodová, M. Sea-level changes and geochemical anomalies across the Cenomanian–Turonian boundary: Pecínov quarry, Bohemia. *Palaeogeogr. Palaeoclim. Palaeoecol.* **1997**, *132*, 265–285. [CrossRef]
7. Wiese, F.; Čech, S.; Ekrt, B.; Košťák, M.; Mazuch, M.; Voigt, S. The Upper Turonian of the Bohemian Cretaceous Basin (Czech Republic) exemplified by the Úpohlavy working quarry: Integrated stratigraphy and paleoceanography of a gateway to the Tethys. *Cretac. Res.* **2004**, *25*, 329–352. [CrossRef]
8. Čech, S.; Hradecká, L.; Svobodová, M.; Švábenická, L. Cenomanian and Cenomanian-Turonian boundary in the southern part of the Bohemian Cretaceous Basin, Czech Republic. *Bull. Geosci.* **2005**, *80*, 321–354.
9. Žítt, J.; Vodrážka, R.; Hradecká, L.; Svobodová, M.; Zágoršek, K. Late Cretaceous environments and communities as recorded at Chrtníky (Bohemian Cretaceous Basin, Czech Republic). *Bull. Geosci.* **2006**, *81*, 43–79. [CrossRef]
10. Vodrážka, R.; Sklenář, J.; Čech, S.; Laurin, J.; Hradecká, L. Phosphatic intraclasts in shallow-water hemipelagic strata: A source of palaeoecological, taphonomic and biostatigraphic data (Upper Turonian, Bohemian Cretaceous Basin). *Cretac. Res.* **2009**, *30*, 204–222. [CrossRef]
11. Al-Bassam, K.S.; Magna, T. Distribution and significance of rare earth elements in Cenomanian-Turonian phosphate components and mudstones from the Bohemian Cretaceous Basin, Czech Republic. *Bull. Geosci.* **2018**, *93*, 347–368. [CrossRef]
12. Košťák, M.; Čech, S.; Uličný, D.; Sklenář, J.; Ekrt, B.; Mazuch, M. Ammonites, inoceramids, and stable carbon isotopes of the Cenomanian-Turonian OAE2 interval in Central Europe: Pecínov quarry, Bohemian Cretaceous Basin (Czech Republic). *Cretac. Res.* **2018**, *87*, 150–173. [CrossRef]
13. Al-Bassam, K.S.; Magna, T.; Vodrážka, R.; Čech, S. Mineralogy and geochemistry of marine glauconitic siliciclasts and phosphates in selected Cenomanian-Turonian units, Bohemian Cretaceous Basin, Czech Republic: Implications for provenance and depositional environment. *Geochemistry* **2019**, *79*, 347–368. [CrossRef]
14. Čech, S.; Hradecká, L.; Laurin, J.; Štaffen, Z.; Švábenická, I.; Uličný, D. Úpohlavy quarry: Record of the late Turonian sea-level oscillations and synsedimentary tectonic activity. In *Stratigraphy and Facies of the Bohemian-Saxonian Cretaceous Basin. Field Trip Guide, 5th International Cretaceous Symposium*; Springer: Berlin/Heidelberg, Germany, 1996; pp. 32–42.
15. Notholt, A.J.G.; Sheldon, R.P.; Davidson, D.F. (Eds.) *Phosphate Deposits of the World: Volume 2, Phosphate Rock Resources*; Cambridge University Press: Cambridge, UK, 1989; pp. 365–368.
16. Decrée, S.; Burlet, C.; Goovaerts, T.; Batista, M.J.; de Oliveira, D.P.S.; Al-Bassam, K.; Malyuk, B.; Coint, N.; McGrath, E.; Bauert, H. Overview of the European phosphate deposits and occurrences: A project dedicated to phosphate mineralizations and associated critical raw materials. In *Proceedings of the SGA Biennial Meeting*; Royal Belgian Institute of Natural Sciences: Brussels, Belgium, 2019.
17. Uličný, D. Depositional systems and sequence stratigraphy of coarse-grained deltas in a shallow-marine, strike-slip setting: The Bohemian Basin, Czech Republic. *Sedimentology* **2001**, *48*, 599–628. [CrossRef]
18. Valečka, J.; Skoček, V. Late Cretaceous lithoevents in the Bohemian Cretaceous Basin, Czechoslovakia. *Cretac. Res.* **1991**, *12*, 561–577. [CrossRef]
19. Čech, S.; Klein, V.; Kříž, J.; Valečka, J. Revision of the Upper Cretaceous stratigraphy of the Bohemian Cretaceous Basin. *Věstn. Ústřed. Ust. Geol.* **1980**, *55*, 277–296.
20. Uličný, D. Sedimentation in a reactivated intra-continental strike-slip fault zone: The Bohemian Cretaceous Basin, Central Europe. *Gaea Heidelb.* **1997**, *3*, 347.
21. Žítt, J.; Nekvasilová, O.; Hradecká, L.; Svobodová, M.; Záruba, B. Rocky coast facies of the Unhost-Tursko High (Late Cenomanian-Turonian, Bohemian Cretaceous Basin). *Acta Musei Natl. Pragae Ser. B Hist. Nat.* **1998**, *54*, 79–116.
22. Vodrážka, R.; Bubík, M.; Švábenická, L.; Žítt, J. Late Cretaceous-Lower Turonian transgressive deposits near Kutná Hora and Kolin (Central Bohemia, Bohemian Cretaceous Basin). In Proceedings of the TMS Foraminifera and Nannofossil Groups Spring Meeting 2013, Prague, Czech Republic, 19–22 June 2013; p. 28.

23. Al-Bassam, K.S.; Halodová, P. Fossil bacteria in Cenomanian–Turonian phosphate nodules and coprolites, Bohemian Cretaceous Basin, Czech Republic. *Ann. Soc. Geol. Pol.* **2018**, *88*, 257–272. [CrossRef]
24. Al-Bassam, K.S. Stable carbon and oxygen isotopes of some carbonate-fluorapatites from Cenomanian and Turonian sequences, Bohemian Cretaceous Basin, Czech Republic. *Iraqi Geol. J.* **2018**, *51*, 1–16.
25. Gulbrandsen, R.A. Relation of carbon dioxide content of apatite of the Phosphoria Formation to regional facies. *Mt. Geol.* **1970**, *8*, 81–84.
26. Dempírová, L.; Šikl, J.; Kašičková, R.; Zoulková, V.; Kříbek, B. The evaluation of precision and relative error of the main components of silicate analyses in Central Laboratory of the Czech Geological Survey. *Geosci. Res. Rep.* **2010**, *43*, 326–330.
27. Ackerman, L.; Magna, T.; Rapprich, V.; Upadhyay, D.; Krátký, O.; Čejková, B.; Erban, V.; Kochergina, Y.U.V.; Hrstka, T. Contrasting petrogenesis of spatially related carbonatites from Samalpatti and Sevattur, Tamil Nadu, India. *Lithos* **2017**, *284–285*, 257–275. [CrossRef]
28. Kechicheda, R.; Laouara, R.; Bruguierc, O.; Laouar-Salmia, S.; Ameur-Zaimecheb, O.; Foufoud, A. Preliminary data REE in Algerian phosphorites: A comparative study and paleo-redox insights. "SYMPHOS 2015", 3rd International Symposium on Innovation and Technology in the Phosphate Industry. *Procedia Eng.* **2016**, *138*, 19–29.
29. Abed, A.M.; Jaber, O.; Alkuisi, M.; Sadaqah, R. Rare earth elements and uranium geochemistry in the Al-Kora phosphorite province, Late Cretaceous, northeastern Jordan. *Arab. J. Geosci.* **2016**, *9*, 187–206. [CrossRef]
30. Aba-Husain, A.; Al-Bassam, K.; Al-Rawi, Y. Rare Earth elements geochemistry of some Paleocene carbonate fluorapatites from Iraq. *Iraqi Bull. Geol. Min.* **2010**, *6*, 81–94.
31. Altschuler, Z.S. The geochemistry of trace elements in marine phosphorites. Part I: Characteristics, abundances and enrichment. *Mar. Phosphorites* **1980**, *29*, 19–30.
32. Wright, J.; Schrader, H.; Holserab, W.T. Paleoredox variations in ancient oceans recorded by rare earth elements in fossil apatite. *Geochim. Cosmochim. Acta* **1987**, *51*, 631–644. [CrossRef]
33. Haskin, M.A.; Haskin, L.A. Rare earths in Europian shales: A redetermination. *Science* **1966**, *154*, 507–509.
34. Zhang, P. Comprehensive recovery and sustainable development of phosphate resources. *Procedia Eng.* **2014**, *83*, 37–51. [CrossRef]
35. Kremer, R.A.; Chokshi, J.C. Fate of rare earths elements in mining/beneficiation of Florida phosphate rocks and conversion to DAP fertilizers. In *Research Report*; Mobile Mining and Minerals Company: Nichols, FL, USA, 1989.
36. Santos, A.J.G.; Mazzilli, B.P.; Favoro, D.I.T. Partitioning of radionuclides and trace elements in phosphogypsum and its source materials based on sequential extraction methods. *J. Environ. Radioact.* **2006**, *87*, 52–61. [CrossRef]
37. Altschuler, Z.S.; Berman, S.; Cuttitta, F. Rare earths in phosphorites-Geochemistry and potential recovery. *USGS Prof. Pap.* **1967**, *575-B*, 125–135.
38. Pereira, F.; Bilal, E. Phosphoric acid extraction and rare earth recovery from apatites of the Brazilian phosphatic ores. *Rom. J. Miner. Depos.* **2012**, *85*, 49–52.
39. Laurino, J.; Mustacato, J. *The Extraction and Recovery of Rare Earth Elements from Phosphate Using PX 107 and Chelok Polymers*; Florida Industrial and Phosphate Research Institute: Bartow, FL, USA, 2015.
40. Barron, E.J.; Thompson, S.L.; Schneder, S.H. A warm, equable Cretaceous: The nature of the problem. *Earth Sci. Rev.* **1983**, *19*, 305–338. [CrossRef]
41. Fletcher, T.L.; Greenwood, D.R.; Moss, P.T.; Salisbury, S.W. Paleoclimate of the Late Cretaceous (Cenomanian-Turonian) portion of the Winton Formation, Central-Western Queensland, Australia: New observations based on CLAMP and Bioclimatic analysis. *Palaios* **2014**, *29*, 121–128. [CrossRef]
42. Bottini, C.; Erba, E. *Paleoclimate and Paleoecology of Calcareous Nannofossils*; EGU General Assembly: Vienna, Austria, 2016.
43. Caracciolo, L.; Pera, L.P.; Muto, F.; Perri, F. Sandstone petrology and mudstone geochemistry ofthe Peruc-Korycany Formation (Bohemian Cretaceous Basin, Czech Republic). *Int. Geol. Rev.* **2011**, *53*, 1003–1031. [CrossRef]
44. Compton, J.; Mallinson, D.; Glenn, C.R.; Fillipelli, G.; Folmi, K.; Shields, G.; Zanin, Y. Variations in the global phosphorus cycle. Marine authegenesis from global to microbial. *Soc. Sedim. Geol. (SEPM) Spec. Publ.* **2000**, *66*, 21–33.
45. Mort, H. Biogeochemical Changes during the Cenomanian–Turonian Oceanic Anoxic Event (OAE 2). Ph.D. Thesis, University of Neuchatel, Neuchâtel, Switzerland, November 2006; p. 197.
46. Glenn, C.R.; Arthur, M.A. Petrology and major element geochemistry of Peru margin phosphorites and associated diagenetic minerals: Authigenesis in modern organic-rich sediments. *Mar. Geol.* **1988**, *80*, 231–267. [CrossRef]
47. Glenn, C.R.; Arthur, M.A. Anatomy and origin of a Cretaceous phosphorite-greensand giant, Egypt. *Sedimentology* **1990**, *37*, 123–154. [CrossRef]
48. Arning, E.T.; Birgel, D.; Brunner, B.; Peckmann, J. Bacterial formation of phosphatic laminites off Peru. *Geobiology* **2009**, *7*, 295–307. [CrossRef] [PubMed]
49. Cosmidis, J.; Benzerara, K.; Menguy, N.; Arning, E. Microscopy evidence of bacterial microfossils in phosphorite crusts of the Peruvian shelf: Implication for phosphogenesis mechanisms. *Chem. Geol.* **2013**, *359*, 10–22. [CrossRef]
50. Hiatt, E.E.; Pufahl, P.K.; Edwards, C.T. Sedimentary phosphate and associated fossil bacteria in a Paleoproterozoic tidal flat in the 1.85Ga Michigamme Formation, Michigan, USA. *Sedim. Geol.* **2015**, *319*, 24–39. [CrossRef]
51. Benmore, R.A.; Coleman, M.L.; McArthur, J.M. Origin of sedimentary francolite from its sulphur and carbon isotope composition. *Nature* **1983**, *302*, 516–518. [CrossRef]
52. Odin, G.S.; Matter, A. Origin of glauconites. *Sedimentology* **1981**, *28*, 611–641. [CrossRef]

53. Amorosi, A. Glaucony and sequence stratigraphy: A conceptual framework of distribution in siliciclastic sequences. *J. Sedim. Res.* **1995**, *65*, 419–425.
54. Arthur, M.A.; Jenkyns, H.C. Phosphorites and paleoceanography. In Proceedings of the 26. International Geological Congress, Paris, France, 7 July 1980; pp. 83–96.
55. De Baar, H.J.W.; Bacon, M.P.; Brewer, P.G. Rare-earth distributions with a positive Ce anomaly in the western North Atlantic Ocean. *Nature* **1983**, *301*, 324–327. [CrossRef]
56. Høgdahl, O.T.; Melsom, S.; Bowen, V.T. Neutron activation analysis of lanthanide elements in seawater. *Am. Chem. Soc.* **1968**, *73*, 308–325.
57. Walaszczyk, I. Mid-Cretaceous events at the marginal part of the Central European Basin (Annopol-on-Vistula section, Central Poland). *Acta Geol. Pol.* **1987**, *37*, 61–74.
58. Ilyn, A. Mid-Cretaceous phosphate platforms of the Russian Craton. *Sediment. Geol.* **1997**, *113*, 125–135. [CrossRef]
59. Carson, G.A.; Crowley, S.F. The glauconite–phosphate association in hardgrounds: Examples from the Cenomanian of Devon, southwest England. *Cretac. Res.* **1993**, *14*, 69–89. [CrossRef]
60. Tzifas, I.T.; Godelitsas, A.; Magganas, A.; Androulakaki, E.; Eleftheriou, G.; Mertzimekis, T.J.; Perraki, M. Uranium-bearing phosphatized limestones of NW Greece. *J. Geochem. Explor.* **2014**, *143*, 62–73. [CrossRef]
61. Tzifas, I.T.; Glasmacher, U.A.; Misaelides, P.; Godelitsas, A.; Gkamaletsos, P.; Goettlicher, J.; de Godoy, D.F. Uranium-bearing francolites present in organic-rich limestones of NW Greece: A preliminary study using synchrotron radiation and fission track techniques. *J. Radioanal. Nucl. Chem.* **2017**, *311*, 465–472. [CrossRef]
62. Al-Bassam, K.S. The Mineralogy and Geochemistry of the Marine Sedimentary Phosphate Deposits of Iraq and other Areas of the East Mediterranean. Ph.D. Thesis, University of Wales, Cardiff, UK, 1974; p. 360.
63. Abed, A.M. The eastern Mediterranean phosphorite giants: An interplay between tectonics and upwelling. *GeoArabia* **2013**, *18*, 67–94.